Heliyon 10 (2024) e30692

Contents lists available at ScienceDirect

Heliyon

journal homepage: www.cell.com/heliyon

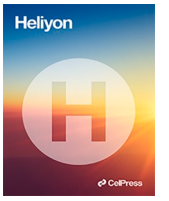

Research article

N-octylpyridine hydrogen sulphate ionic liquid for multifunctional fluorescent response in different solvents

Peng Tian [a,**], Jian Shao [a], Yanhong Kang [a], Si-Si Zhao [a,***], Yajun Fu [a], Dan Wu [b], Hang Zhang [a,*]

[a] College of Chemistry & Chemical Engineering, Shenyang Normal University, Shenyang, Liaoning, 110034, PR China
[b] Laboratory Centre of Shenyang Normal University, Shenyang, Liaoning, 110034, PR China

ARTICLE INFO

Keywords:
Ionic liquid
Fluorescence spectrum
$[OP]HSO_4$
Multifunctional fluorescent response

ABSTRACT

Ionic liquids (ILs) have attracted considerable interest in the last two decades owing to their unique fluorescent properties. Herein, N-octylpyridine hydrogen sulphate ($[OP]HSO_4$) was synthesised and characterised using ^1H NMR and infrared spectroscopies. In addition, the fluorescence spectra of $[OP]HSO_4$ in water, methanol, ethanol and acetonitrile were studied. In a single solvent, as the concentration of the solvent (methanol, ethanol or acetonitrile) increases, the fluorescence intensity of the IL first increases and then decreases. A similar trend was observed in their mixed solvents with water. Moreover, the fluorescence intensity of $[OP]HSO_4$ decreases with increasing temperature. A fluorescence intensity reduction of only 4.46% for $[OP]HSO_4$ after continuous scanning for 40 cycles under the maximum excitation state was analysed. The lack of photobleaching observed in $[OP]HSO_4$ indicates its good photobleaching resistance.

1. Introduction

Ionic liquids (ILs) are molten salts that are liquid at room temperature [1,2] and exhibit unique properties, such as low vapour pressure [3], high thermal stability [4,5] and good electrical conductivity [6–8], which offer broad application prospects [9–11]. Compared with the traditional volatile organic solvents, they have a negligible vapour pressure, making them 'green' solvents. Because of these characteristics, ILs are used as alternative electrolytes in lithium-ion batteries and double-layer capacitors [12,13]. ILs are widely used in analytical chemistry applications, such as highly polar capillary columns that can separate complex mixtures in gas chromatography [14] and mobile-phase additives in liquid chromatography [15]. ILs have different responses and diverse application performances, characterised using infrared [16], ultraviolet [17] and fluorescence [18] spectroscopies. Notably, fluorescent ILs exhibit stimulus responsiveness, chirality or prominent optical properties, which greatly broaden their application prospects [19].

Compared with common fluorescent organic molecules, fluorescent ILs exhibit obvious advantages in terms of regulating optical properties [20]. There are two main aspects in the study of ILs for fluorescence spectroscopic detection. First, the fluorescence properties of ILs combined with other substances are used for specific detection. ILs with symmetrical structures have higher fluorescence quantum yield owing to the enhanced π–π* conjugation. Owing to the excellent hydrophilicity and strong fluorescence

* Corresponding author.
** Corresponding author.
*** Corresponding author.
E-mail addresses: tianpenglnu@sina.com (P. Tian), zhaoss@synu.edu.cn (S.-S. Zhao), zhangh@synu.edu.cn (H. Zhang).

https://doi.org/10.1016/j.heliyon.2024.e30692
Received 2 February 2024; Received in revised form 30 April 2024; Accepted 2 May 2024
Available online 3 May 2024

properties of some ILs, they are expected to be novel fluorescent probes [21,22] with high selectivity and sensitivity in the sensing and detection of biomacromolecules [23], oil field development [24], electrochemistry [25], medicine [26] and other directions. Gan found that due to the tunability of ILs, a new fluorescent IL probe [P66614][HQS] was designed, synthesised and characterised owing to the introduction of specific fluorophores into ILs. The new fluorescent IL probe [P66614][HQS] has a unique performance as a chemical sensor for the detection of Al^{3+} in aqueous solutions [27]. Second, fluorescent properties are used to judge the functional groups and structures of new ILs [28,29]. ILs can also be used as organic solvents for the fluorescence spectrometric determination of different substances [30]. Owing to their unique physical and chemical properties, they can enhance the fluorescence properties of other substances [31]. An abnormal absorption and fluorescence behaviour has been reported for ILs in the visible light range. The fluorescence spectra of ILs vary with the excitation wavelength, and the aggregation structure of ILs can be used to explain this unique phenomenon [32]. Meanwhile, with the increase in excitation wavelength, the fluorescence from these ILs continuously undergoes a red shift [33]. Burrel et al. [34] reported that the fluorescence intensity of a pyrrolidine IL would be greatly reduced after the systematic purification of the intermediate in the synthesis process. However, heating it above 150 °C increases absorption and fluorescence in the visible light range, similar to heating imidazole ILs above 150 °C. Moreover, the fluorescence intensity has been related to polarity [35], temperature [36,37], pH value [38,39] and others [40,41].

In this research, a pyrrolidine IL, N-octylpyridine hydrogen sulphate [OP]HSO_4 (Scheme 1), was prepared. The influences of [OP]HSO_4 concentration and temperature on the fluorescence performance of the IL in single and mixed solvents are discussed in detail. The photobleaching resistance of [OP]HSO_4 was also examined.

2. Materials and methods

2.1. Materials and reagents

All reagents were purchased from Tian Jin Fuyu Fine Chemical Co., Ltd. The system used to produce distilled water was the SAS67120 model ultrapure water purifier.

2.2. Synthesis of N-octyl pyridine hydrogen sulphate intermediates ([OP]Br)

A mixture of bromo-*n*-octane (173.7 mL, 1 mol) and pyridinium (96.6 mL, 1.2 mol) was added in a 500-mL round-bottom flask with stirring for heating reflux at 117 °C, the resulting solution immediately turned brown–yellow. After heating for a period, a small amount of brownish oil droplets appeared at the bottom of the flask. The reflux was continued for 48 h, forming numerous dark brown oil droplets. Upon completion of the reaction, the mixture was allowed to cool, leading to the precipitation of brown crystals. The crude product [OP]Br was obtained using vacuum filtration. It was subsequently mixed with a small amount of the organic solvent CH_3CN and heated for approximately 20 min. After discontinuing the heating, the mixture was left to cool for crystallisation, followed by vacuum filtration. To obtain a purer IL, the process was repeated three times by recrystallising with CH_3CN. The intermediate [OP]Br was promptly bottled and stored in a vacuum desiccator for further use. The yield of [OP] Br was 72% [42] (Scheme 1). Using 10 μL of DMSO as an internal standard, [OP] Br was placed in an NMR tube, and ^{1}H NMR was performed at room temperature (Fig. S1). ^{1}H NMR (500 MHz, DMSO-d_6): δ 9.27 (d, J = 6.0 Hz, 2H, Pyridine–$H_{2,6}$), 8.82 (t, J = 8.0 Hz, 1H, Pyridine–H_4), 8.35 (t, J = 7.0 Hz, 2H, Pyridine–$H_{3,5}$), 4.93 (t, J = 7.5 Hz, 2H, N–CH_2), 2.20 (m, 2H, N–CH_2CH_2), 1.28–1.50 (m, 10H, N–CH_2CH_2) and 0.86 (t, J = 6.5 Hz, 3H, –CH_3) ppm.

2.3. Synthesis of N-octyl pyridine hydrogen sulphate ([OP]HSO_4)

[OP]Br (27.2 g, 0.1 mol) was dissolved in 30 mL dichloromethane and placed into an iodine flask, followed by the addition of sulfuric acid (0.1 mol, 5.43 mL). Continuous stirring for 24 h resulted in the formation of a brown oily liquid upon settling. Finally, residual solvents were removed upon vacuum distillation to obtain a transparent, viscous IL, [OP]HSO_4 (Scheme 1). The yield of [OP]HSO_4 was 82%. Using 10 μL of DMSO as an internal standard, [OP]HSO_4 was placed in an NMR tube, and ^{1}H NMR was performed at room temperature. ^{1}H NMR (500 MHz, DMSO-d_6): δ 9.12 (d, J = 4.5 Hz, 2H, Pyridine–$H_{2,6}$), 8.61 (t, J = 6.5 Hz, 1H, Pyridine–H_4), 8.17 (t, J = 6.0 Hz, 2H, Pyridine–$H_{3,5}$), 4.61 (t, J = 6.5 Hz, 2H, N–CH_2), 1.91 (m, 2H, N–CH_2CH_2), 1.26 (m, 10H, N–CH_2CH_2) and 0.85 (t, J = 6.0 Hz, 3H, –CH_3) ppm (see Fig. 1).

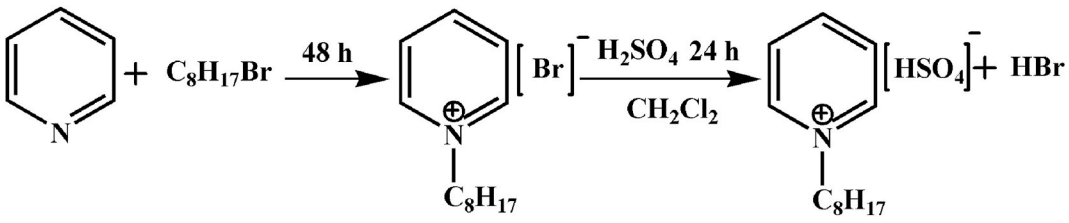

Scheme 1. Schematic of the preparation of [OP]HSO_4.

2.4. Experimental equipment and analytical instruments

The experimental equipment included the ISO9001 electronic balance, 10-mm quartz colourimetric dish, 10–100 μL pipet gun, KQ3200 ultrasonic cleaner, Model 202-1 electric thermostatic drying oven and 98-1-B electronic control heating mantle. Fluorescent spectra were collected using a fluorescence spectrophotometer (Agilent Cary Eclipse) with a Xenon flash lamp pulsed at 80 Hz. FTIR spectra were measured on a Mattson Alpha Centauri spectrometer at room temperature. The IL was analysed using ^{1}HNMR on a 500-MHz Bruker Avance III NMR spectrometer.

2.5. Preparation of single-solvent solutions

[OP]HSO_4 (0.1500 g) was dissolved in a small amount of water, methanol, ethanol and acetonitrile and then transferred to a 50-mL volumetric flask, and water, acetonitrile, ethanol and methanol were added to have a constant volume to prepare a standard solution. The standard solutions were diluted to 25, 50, 150, 300 and 400 μg/mL for fluorescence experiments.

2.6. Preparation of mixed-solvent solutions

Mixed-solvent [OP]HSO_4 solutions (300 μg/mL) were prepared as follows: The water:acetonitrile, water:ethanol, and water: methanol volume ratios were 1:9, 2:8, 3:7, 4:6, 5:5, 6:4, 7:3, 8:2 and 9:1.

2.7. Measurement at different temperatures

300-μg/mL [OP]HSO_4 solutions with water, methanol, ethanol and acetonitrile were heated up to 60 °C in the oven, followed by cooling to 50 °C, 35 °C, 25 °C and 20 °C. Their fluorescence spectra were measured using a colourimetric dish.

3. Results and discussion

To verify the synthesis of [OP]HSO_4, IR spectroscopy was used (Fig. 2). The positions of each characteristic peak can be obtained as follows: the expansion and contraction vibration peak of C–H bonds on the pyridine ring; C=C bond bending vibrations on the pyridine ring; octyl-saturated C–H bond stretching vibration peak: 2960 and 2860 cm^{-1}; octyl upper methylene curve vibration peak: 1490 cm^{-1}. Compared with the raw materials, [OP]HSO_4 increases the stretching and deformation vibrations of methyl groups, while the skeletal vibrations of pyridine are still present. The synthesis and purification process combined with [OP]HSO_4 and the position of the IR characteristic peak were within the allowable error range, confirming the successful synthesis of [OP]HSO_4.

3.1. Effects of single solvents on the fluorescence intensity of [OP]HSO_4

The excitation wavelength (λex) of [OP]HSO_4 in water, methanol, ethanol and acetonitrile was 225 nm. Under the same excitation wavelength, the maximum emission wavelengths (λem) of [OP]HSO_4 in water, methanol, ethanol and acetonitrile were 349, 292, 354

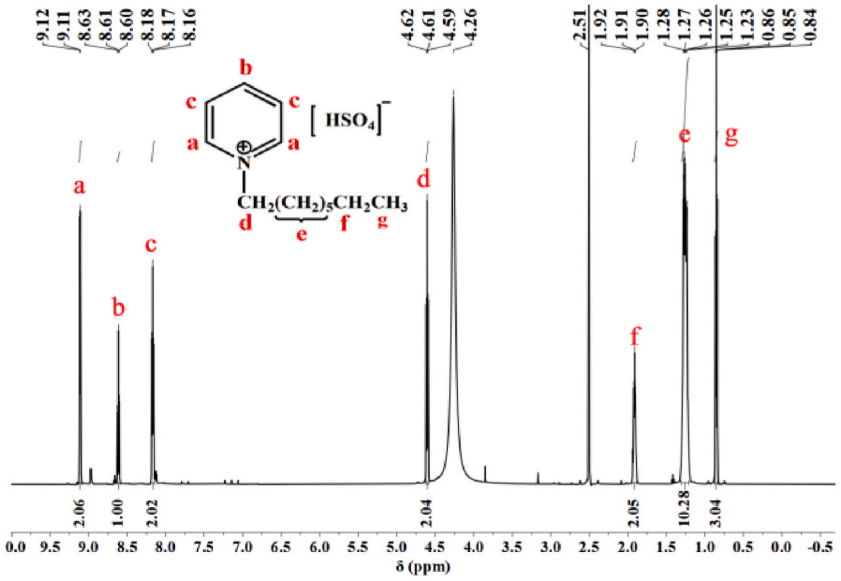

Fig. 1. ^{1}H NMR of [OP]HSO_4.

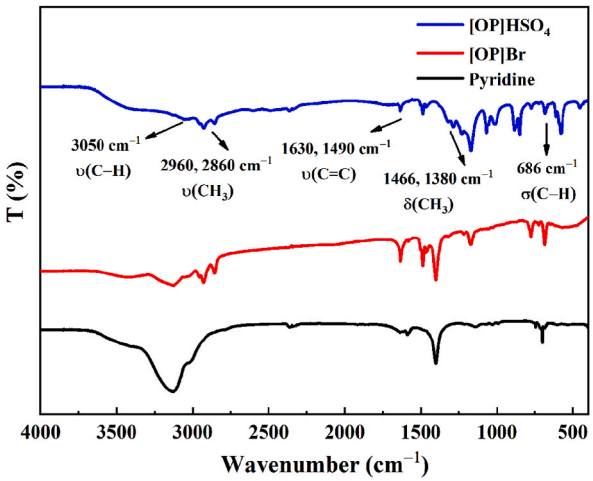

Fig. 2. IR spectra of pyridine, [OP]Br and [OP]HSO_4.

and 354 nm, respectively (Fig. 3) The fluorescence intensity: methanol > ethanol > acetonitrile > water. The fluorescence intensity of [OP]HSO_4 is affected by the type of solvent, and the position and strength of λem are different in different solvents. In general, the larger the dipole moment, the stronger the polarity. The polarity order of solvents is as follows: water > methanol > ethanol > acetonitrile [43].

The effects of solvent on fluorescence intensity can be classified into general solvent effects and special solvent effects. General effects are related to the electronic polarisation, which is determined by the refractive index of the medium, and the molecular polarisation, determined by the static dielectric constant [44]. The latter comprises all these local interactions, such as hydrogen bonding, charge transfer, proton transfer, etc. The shift value of the fluorescence spectrum caused by special solvent effects is often greater than that caused by general solvent effects. Owing to interactions between the IL and solvent molecules, the fluorescence spectra of the same fluorescent substance in different solvents may considerably differ. In addition, the shape of the emission peak of the compound substantially changed in different solvents. The IL exhibits a double-fluorescence phenomenon, such as MOFs and other molecules [45].

3.2. *Effects of mixed solvents on the fluorescence intensity of [OP]HSO_4*

The fluorescence results of [OP]HSO_4 in water–methanol, water–ethanol and water–acetonitrile mixed solvents were obtained. In the mixed solvents, the fluorescence intensity first increased and then decreased. The fluorescence intensity of [OP]HSO_4 reached the maximum when the acetonitrile volume fraction was 84% (Fig. 4), the ethanol volume fraction was 72% (Fig. 5) and the methanol volume fraction was 76% (Fig. 6). Subsequently, the fluorescence intensity of [OP]HSO_4 decreased. This is because the ability of [OP]HSO_4 to form hydrogen bonds with water is stronger than that with acetonitrile, ethanol and methanol, resulting in a more stable configuration of [OP]HSO_4 in aqueous solution, low radiative transition efficiency and relatively small fluorescence intensity as it is

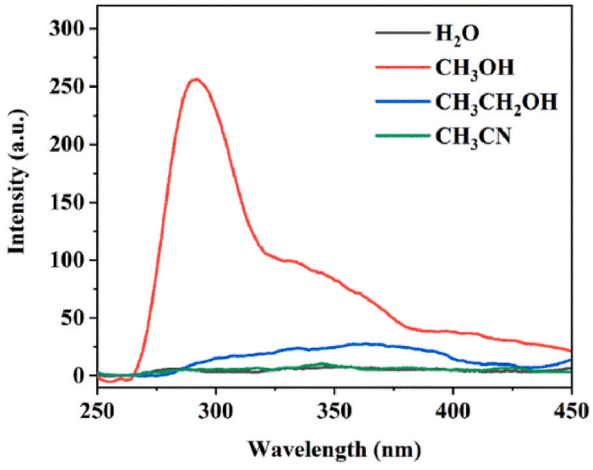

Fig. 3. Fluorescence emission spectra of [OP]HSO_4 in water, methanol, ethanol and acetonitrile.

directly proportional to the radiative efficiency. When acetonitrile, ethanol and methanol are mixed with water, with the decrease in water content, the ability of the solute to form hydrogen bonds with the solvent weakens, the stability of $[OP]HSO_4$ decreases, the ability of radiative transition begins to increase, and the fluorescence intensity increases. When the volume fraction of acetonitrile, ethanol and methanol in the mixed solution was more than 84%, 72% and 76%, respectively, the ability to form hydrogen bonds between the IL and acetonitrile, ethanol and methanol was enhanced, which improved the stability of the IL and decreased the fluorescence intensity [46].

3.3. Effects of concentration on the fluorescence intensity of $[OP]HSO_4$

Fig. 7 (a) and 7 (b) show the relation between the concentration of $[OP]HSO_4$ in acetonitrile. As the concentration increases, the fluorescence intensity decreases. However, as the concentration of the IL in methanol (Fig. 8 (a) and 8 (b)), ethanol (Fig. 9 (a) and 9 (b)) and water (Fig. 10 (a) and 10 (b)) increases, the fluorescence intensity decreases, the fluorescence intensity decreases s for ethanol and methanol, the fluorescence intensity is as follows: with the gradual increase of the concentration of ILs, the relation between the fluorescence intensity and the concentration develops from linear to lost linear. Even when the concentration exceeds a certain value, the fluorescence intensity decreases owing to the relation between the concentration and fluorescence intensity as follows:

$$I_f = 2.303 Y_f I_0 \varepsilon b c, \tag{1}$$

where I_f is the fluorescence intensity, Y_f is the fluorescence quantum yield, I_0 is the intensity of incident light and ε is the light absorption coefficient. At low concentrations, I_f is proportional to c. Moreover, the IL concentration affects fluorescence. Higher concentrations may cause molecular interactions, self-quenching, or aggregation effects [47]. When the concentration is too high, the probability of intermolecular collision increases and energy transfer occurs between the emission and absorption spectra, resulting in an overlap. The intensity of excitation light is weakened owing to the strong absorption of incident light by $[OP]HSO_4$ solution with a large concentration, and the efficiency of radiation transition is reduced, leading to a decrease in fluorescence intensity.

3.4. Effects of temperature on the fluorescence intensity of $[OP]HSO_4$

Temperature affects molecular mobility, viscosity, and nonradiative processes, altering the fluorescence intensity and duration of ILs. The fluorescence intensity of ILs remains relatively stable in acetonitrile, ethanol, methanol and water (Figs. 11–14, respectively). The fluorescence intensity of $[OP]HSO_4$ showed a slight downward trend with the increase in temperature. The reason for this phenomenon is that the viscosity of $[OP]HSO_4$ is inversely proportional to the temperature [48]. The increase in temperature and the decrease in viscosity increase the chance of collisions between $[OP]HSO_4$ and solvent molecules, resulting in the transfer of the energy in the excited state to solvent molecules or the loss of energy in the form of heat, which improves the probability of internal conversion and decreases the fluorescence intensity.

3.5. Photobleaching resistance of $[OP]HSO_4$

A 300-μg/mL $[OP]HSO_4$ aqueous solution was exposed to the maximum excitation state and scanned continuously for 0, 10, 20, 30 and 40 cycles. As can be seen from Table 1, the fluorescence intensity tended to be stable after scanning for 20 cycles (length of one scan was 25 s). By calculating the reduction of the maximum emission peak area before and after scanning, we found that the fluorescence intensity declined by 4.46%. The fluorescence intensity of $[OP]HSO_4$ decreases gradually with the increase in scanning cycles under the maximum excitation state. The lack of photobleaching indicates that $[OP]HSO_4$ has good photobleaching resistance.

3.6. Fluorescence quantum yield of $[OP]HSO_4$

The value of the fluorescence quantum yield represents the fluorescence intensity, which directly affects the properties of the

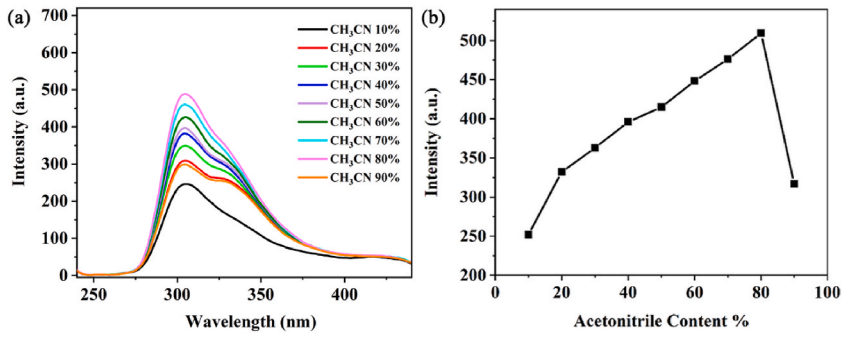

Fig. 4. Water–acetonitrile fluorescence spectra (a) and fluorescence intensity versus acetonitrile content (b) of $[OP]HSO_4$.

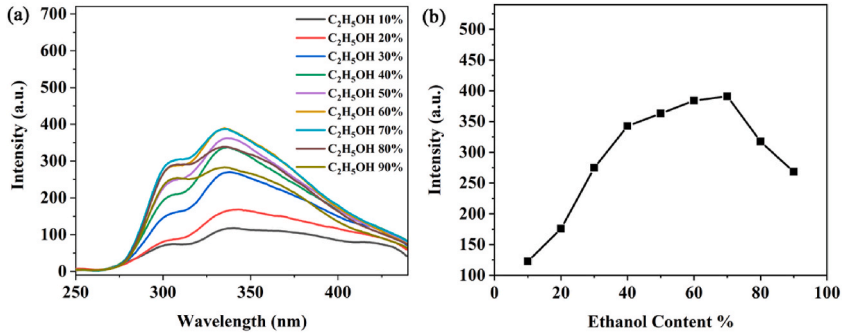

Fig. 5. Water–ethanol fluorescence spectra (a) and fluorescence intensity versus ethanol content (b) of $[OP]HSO_4$.

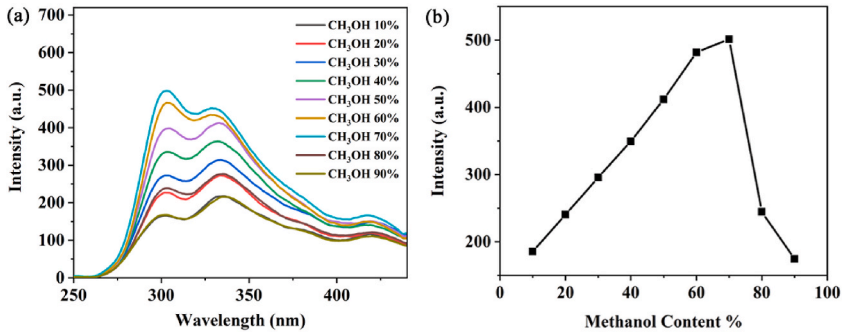

Fig. 6. Water–methanol fluorescence spectra (a) and fluorescence intensity versus methanol content (b) of $[OP]HSO_4$.

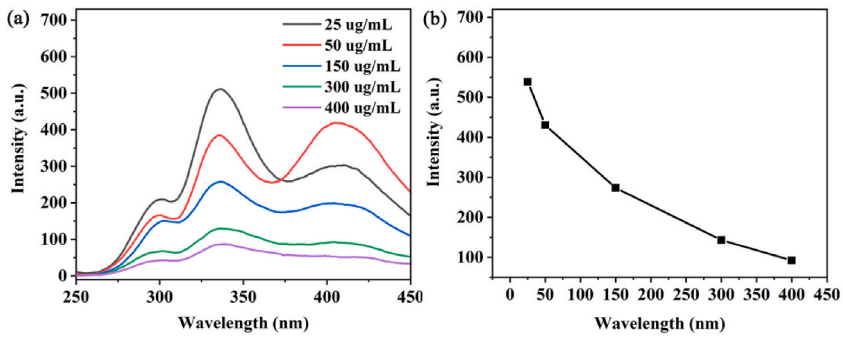

Fig. 7. Fluorescence spectra collected at various concentrations (a) and fluorescence intensities (b) of $[OP]HSO_4$ in acetonitrile.

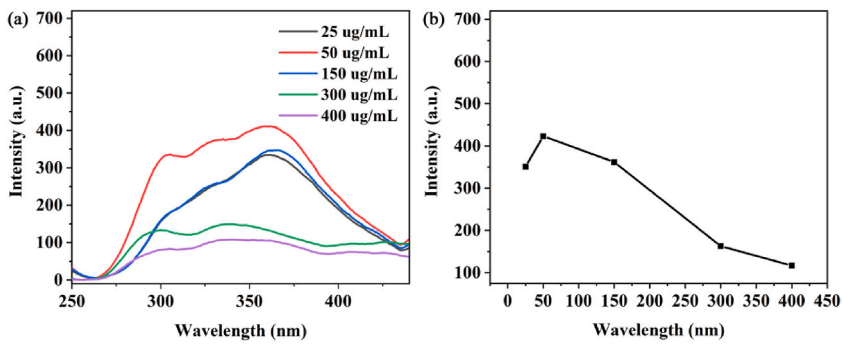

Fig. 8. Fluorescence spectra collected at various concentrations (a) and fluorescence intensities (b) of $[OP]HSO_4$ obtained in ethanol.

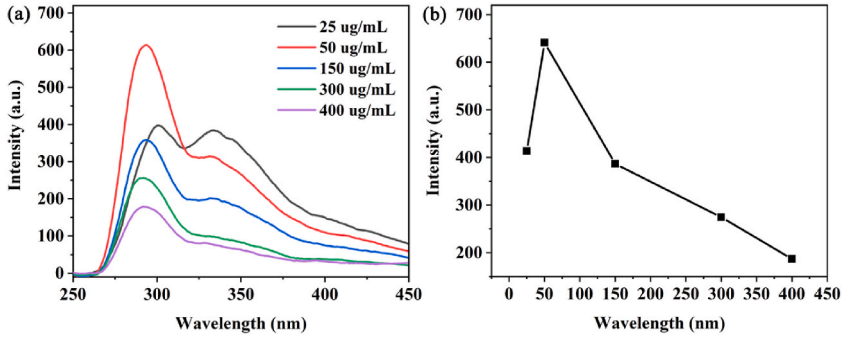

Fig. 9. Fluorescence spectra collected at various concentrations (a) and fluorescence intensities (b) of $[OP]HSO_4$ obtained in methanol.

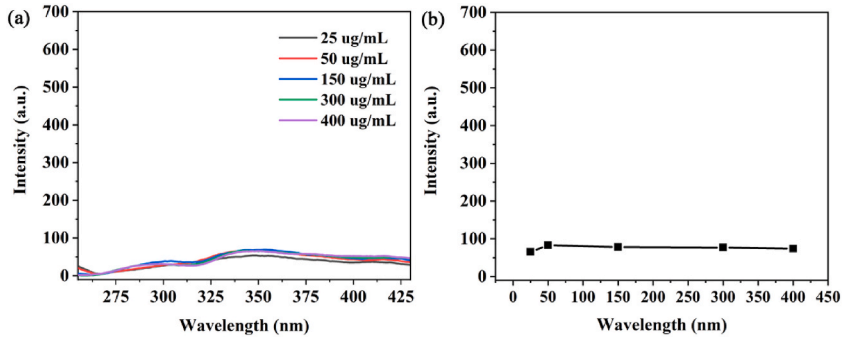

Fig. 10. Fluorescence spectra collected at various concentrations (a) and fluorescence intensities (b) of $[OP]HSO_4$ obtained in water.

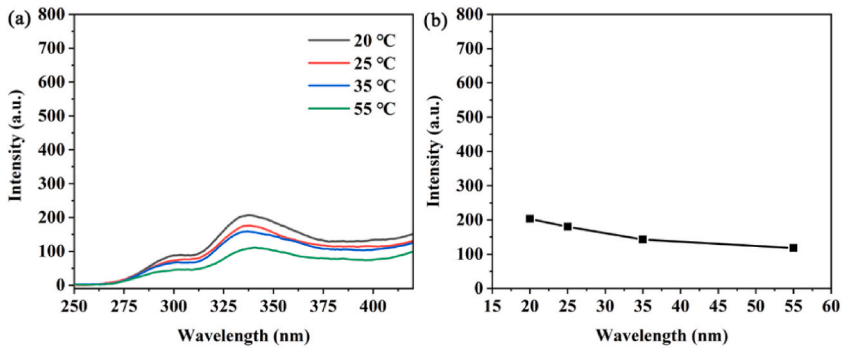

Fig. 11. Fluorescence spectra collected at various temperatures (a) and fluorescence intensity versus wavelength (b) for $[OP]HSO_4$ in acetonitrile.

material. Using the reference method, 5-μg/mL ethanol solutions of $[OP]HSO_4$ and Rhodamine B were removed to measure the UV spectra of the two, and their absorbance at the same wavelength was recorded. The fluorescence emission spectra of the same solutions were measured on a fluorescence spectrophotometer (λ_{ex} = 225 nm was used as the excitation wavelength).

$$\varnothing \mathbf{u} = \varnothing \mathbf{s} \bullet \frac{\boldsymbol{Yu}}{\boldsymbol{Ys}} \bullet \frac{\boldsymbol{As}}{\boldsymbol{Au}}, \tag{2}$$

where Φu is the fluorescence quantum yield of the material, Φs is the fluorescence quantum yield of the standard substance, *Yu* is the fluorescence integral area of the material, *Ys* is the fluorescence integral area of the reference material, *Au* is the absorbance of the ultraviolet incident light of the material and *As* is the ultraviolet absorbance of the reference material. As shown in Table 2, the fluorescence quantum yield of $[OP]HSO_4$ in ethanol was calculated as 0.46 by substituting these values into Equation (2).

4. Conclusions

Herein, $[OP]HSO_4$ was synthesised and characterised using ^1H NMR and infrared spectroscopies. The fluorescence spectra of [OP]

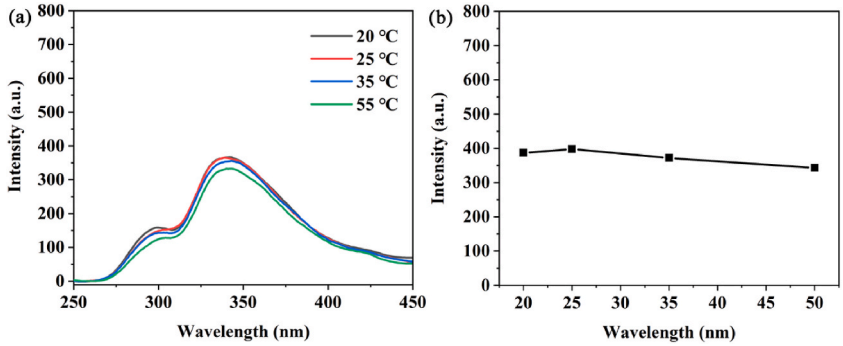

Fig. 12. Fluorescence spectra collected at various temperatures (a) and fluorescence intensity versus wavelength (b) for [OP] HSO_4 in ethanol.

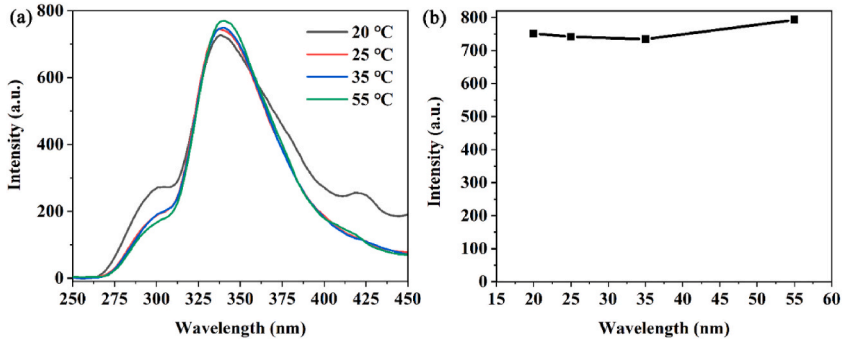

Fig. 13. Fluorescence spectra collected at various temperatures (a) and fluorescence intensity versus wavelength (b) for [OP]HSO_4 in methanol.

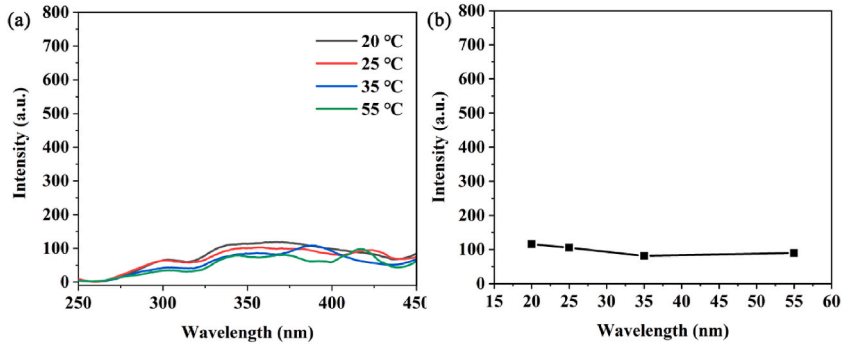

Fig. 14. Fluorescence spectra collected at various temperatures (a) and fluorescence intensity versus wavelength (b) for [OP]HSO_4 in water.

Table 1
[OP]HSO_4 scan times and fluorescence intensity relation in water.

Scan times	0	10	20	30	40
Fluorescence intensity	241.02	229.61	226.67	226.44	225.8
Peak area	31735.5	30423.2	30348.4	30321.1	30319.1

Table 2
[OP]HSO_4 scan cycle–fluorescence intensity relation in ethanol.

Yu	Ys	Au	As	Φs	Φu
22983.1	32606.4	0.0298	0.0200	0.97	0.46

HSO_4 in water, methanol, ethanol and acetonitrile were studied. The different fluorescence effects produced in the solvents may be attributed to the combined influence of general and special solvent effects. In addition, in the mixed solutions, the fluorescence intensity presents an increasing trend, followed by a decrease attributed to changes in the strength of hydrogen bonds between the solvents, IL, and water. The fluorescence intensity of the IL first increases and then decreases, changing from linear to nonlinear under a single solvent. Moreover, the fluorescence intensity of $[OP]HSO_4$ exhibited a slight decrease with increasing temperature owing to changes in viscosity. The fluorescence intensity loss of only 4.46% obtained for $[OP]HSO_4$ after continuous scanning for 40 cycles under the maximum excitation state was analysed. The lack of obvious photobleaching indicates that $[OP]HSO_4$ has good photobleaching resistance.

Ethical approval

No experiments were carried out involving human tissue.

Data availability statement

No data was used for the research descried in the article.

CRediT authorship contribution statement

Peng Tian: Investigation. **Jian Shao:** Investigation. **Yanhong Kang:** Data curation. **Si-Si Zhao:** Writing – review & editing. **Yajun Fu:** Formal analysis. **Dan Wu:** Validation. **Hang Zhang:** Writing – review & editing.

Declaration of competing interest

The authors declare that they have no known competing financial interests or personal relationships that could have appeared to influence the work reported in this paper.

Acknowledgements

Basic Scientific Research Project of Colleges and Universities of Liaoning Province Education Department (Grant No. JYTMS20231693) and the National Naturnal Science Foundation of China (Grant No. 22109105, 22102106) are gratefully acknowledged.

Appendix B. Supplementary data

Supplementary data to this article can be found online at https://doi.org/10.1016/j.heliyon.2024.e30692.

References

[1] R.D. Rogers, K.R. Seddon, Ionic liquids—solvents of the future? Science 302 (5646) (2003) 792–793, https://doi.org/10.1126/science.1090313.
[2] M. Freemantle, An Introduction to Ionic liquids[M], Royal Society of chemistry, 2010.
[3] S. Ravula, N.E. Larm, M.A. Mottaleb, M.P. Heitz, G.A. Baker, Vapor pressure mapping of ionic liquids and low-volatility fluids using graded isothermal thermogravimetric analysis, ChemEngineering 3 (2) (2019) 42, https://doi.org/10.3390/chemengineering3020042.
[4] C. Maton, N.D. Vos, C.V. Stevens, Ionic liquid thermal stabilities: decomposition mechanisms and analysis tools, Chem. Soc. Rev. 42 (2013) 5963–5977, https://doi.org/10.1039/C3CS60071H.
[5] L. Chancelier, A.O. Diallo, C.C. Santini, G. Marlair, T. Gutel, S. Mailley, C. Len, Targeting adequate thermal stability and fire safety in selecting ionic liquid-based electrolytes for energy storage, Phys. Chem. Chem. Phys. 16 (2014) 1967–1976, https://doi.org/10.1039/C3CP54225D.
[6] T.E. Karakasidis, F. Sofos, C. Tsonos, The electrical conductivity of ionic liquids: numerical and analytical machine learning approaches, Fluid 7 (10) (2022) 321, https://doi.org/10.3390/fluids7100321.
[7] E. Rodil, A. Arce, A. Arce, A. Soto, Measurements of the density, refractive index, electrical conductivity, thermal conductivity and dynamic viscosity for tributylmethylphosphonium and methylsulfate based ionic liquids, Thermochim. Acta 664 (2018) 81–90, https://doi.org/10.1016/j.tca.2018.04.007.
[8] G. Chen, N. Chen, L. Li, Q. Wang, W.F. Duan, Ionic liquid modified poly(vinyl alcohol) with improved thermal processability and excellent electrical conductivity, Ind. Eng. Chem. Res. 57 (2018) 5472–5481, https://doi.org/10.1021/acs.iecr.8b00157.
[9] K. Yavir, K. Konieczna, Ł. Marcinkowski, A. Kloskowski, Ionic liquids in the microextraction techniques: the influence of ILs structure and properties, TrAC, Trends Anal. Chem. 130 (2020) 115994, https://doi.org/10.1016/j.trac.2020.115994.
[10] G. Choudhary, J. Dhariwal, M. Saha, S. Trivedi, M.K. Banjare, R. Kanaoujiya, Ionic liquids: environmentally sustainable materials for energy conversion and storage applications, Environ. Sci. Pollut. Control Ser. 31 (7) (2024) 10296–10316, https://doi.org/10.1007/s11356-023-25468-w.
[11] S.V. Muginova, D.A. Myasnikova, S.G. Kazarian, T.N. Shekhovtsova, Applications of ionic liquids for the development of optical chemical sensors and biosensors, Anal. Sci. 33 (3) (2017) 261–265, https://doi.org/10.2116/analsci.33.261.
[12] Q.W. Yang, Z.Q. Zhang, X.-G. Sun, Y.-S. Hu, H.B. Xing, S. Dai, Ionic liquids and derived materials for lithium and sodium batteries, Chem. Soc. Rev. 47 (2018) 2020–2064, https://doi.org/10.1039/C7CS00464H.
[13] M. Watanabe, M.L. Thomas, S.G. Zhang, K. Ueno, T. Yasuda, K. Dokko, Application of ionic liquids to energy storage and conversion materials and devices, Chem. Rev. 117 (2017) 7190–7239, https://doi.org/10.1021/acs.chemrev.6b00504.

[14] M.V. Shashkov, V.N. Sidelnikov, A.A. Bratchikova, O.A. Nikolaeva, New dicationic quinolinium ionic liquids for capillary gas chromatography, Russ. J. Phys. Chem. A 94 (2020) 1494–1502, https://doi.org/10.1134/s0036024420070262.
[15] Z.J. Yin, Y.N. Zhang, F.J. Guan, H. Yu, Y.J. Ma, Simultaneous separation and indirect ultraviolet detection of chlorate and perchlorate by pyridinium ionic liquids in reversed-phase liquid chromatography, J. Separ. Sci. 43 (2020) 3868–3875, https://doi.org/10.1002/jssc.202000690.
[16] A.S. Shalygin, N.S. Nesterov, S.A. Prikhod'ko, N.Y. Adonin, O.N. Martyanov, S.G. Kazarian, Interactions of CO2 with the homologous series of CnMIMBF4 ionic liquids studied in situ ATR-FTIR spectroscopy: spectral characteristics, thermodynamic parameters and their correlation, J. Mol. Liq. 315 (2020) 113694–113705, https://doi.org/10.1016/j.molliq.2020.113694.
[17] P.Q. Li, S. Tan, Y. Wu, C.H. Wang, M. Watanabe, Azobenzene-Based ionic liquid switches phase separation of poly(N-isopropylacrylamide) aqueous solutions as a molecular trigger, leading to UV shutdown of ionic transport, ACS Macro Lett. 9 (2020) 825–829, https://doi.org/10.1021/acsmacrolett.0c00170.s001.
[18] D.W. Zhang, Y.P. Wang, J.C. Xie, W.P. Geng, H.L. Liu, Ionic-liquid-stabilized fluorescent probe based on S-doped carbon dot-embedded covalent-organic frameworks for determination of histamine, Microchim. Acta 187 (2019) 28–36, https://doi.org/10.1007/s00604-019-3833-7.
[19] X.Q. Yuan, Y.Q. Zhang, Z.Y. Li, F. Huo, Y.H. Dong, H.Y. He, Stimuli-responsive ionic liquids and the regulation of aggregation structure and phase behavior, Chin. J. Chem. 39 (3) (2021) 729–744, https://doi.org/10.1002/cjoc.202000414.
[20] A. Paul, P.K. Mandal, A. Samanta, On the optical properties of the imidazolium ionic liquids, J. Phys. Chem. C (2005) 9148–9153, https://doi.org/10.1021/jp0503967.
[21] J. Harathi, K. Thenmozhi, Water-soluble ionic liquid as a fluorescent probe towards distinct binding and detection of 2,4,6-trinitrotoluene and 2,4,6-trinitrophenol in aqueous medium, Chemosphere 286 (2022) 195–202, https://doi.org/10.1016/j.chemosphere.2021.131825.
[22] H. Liu, L. Zhang, J. Chen, Y. Zhai, Y. Zeng, L. Li, A novel functional imidazole fluorescent ionic liquid: simple and efficient fluorescent probes for superoxide anion radicals, Anal. Bioanal. Chem. 405 (2013) 9563–9570, https://doi.org/10.1007/s00216-013-7357-4.
[23] L.S. Li, Z.G. Tai, X.Y. Wu, J.C. Wu, T.R. Zhang, Z.J. Chen, Q.Z. Zhu, Ionic liquids: momentous tools in transdermal delivery of biomacromolecules, Advanced Therapeutics 6 (6) (2023) 2200332, https://doi.org/10.1002/adtp.202200332.
[24] J.S. Sun, Z.Y. Xiu, L. Li, L.V. Kaihe, X.F. Zhang, Z.L. Wang, Z.W. Dai, Z. Xu, N. Huang, J.P. Liu, Application status and prospect of ionic liquids in oilfield chemistry, Petroleum (2023), https://doi.org/10.1016/j.petlm.2023.08.001.
[25] G.A.O. Tiago, I.A.S. Matias, A.P.C. Ribeiro, L.M.D.R.S. Martins, Application of ionic liquids in electrochemistry—recent advances, Molecules 25 (24) (2020) 5812, https://doi.org/10.3390/molecules25245812.
[26] S. Chandel, A.R. Pathania, An insight into the advances in ionic liquids and its applications in medicine, Mater. Today: Proc. (2023), https://doi.org/10.1016/j.matpr.2023.09.105.
[27] L. Gan, J. Guo, S. Che, Q. Xiao, M. Wang, J. You, C. Wang, Design of functionalized fluorescent ionic liquid and its application for achieving significant improvements in Al3+ detecting, Green Energy Environ. 5 (2020) 195–202, https://doi.org/10.1016/j.gee.2020.03.006.
[28] G. Tang, J.F. Niu, W.B. Zhang, J.L. Yang, J.Y. Tang, R. Tang, Z.Y. Zhou, J.Q. Li, Y.S. Cao, Preparation of acifluorfen-based ionic liquids with fluorescent properties for enhancing biological activities and reducing the risk to the aquatic environment, J. Agric. Food Chem. 68 (2020) 6048–6057, https://doi.org/10.1021/acs.jafc.0c00842.
[29] B. James, C.P. Butts, P.J. Martin, M.C. Vergara-Gutierrez, Aggregation behavior of aqueous solutions of ionic liquids, Langmuir: the ACS journal of surfaces and colloidsr 20 (2004) 2191–2198, https://doi.org/10.1021/la035940m.
[30] C.F. Poole, S.K. Poole, Extraction of organic compounds with room temperature ionic liquids, J. Chromatogr. A 1217 (2010) 2268–2286, https://doi.org/10.1016/j.chroma.2009.09.011.
[31] H. Wu, L. Zhang, L.M. Du, Ionic liquid sensitized fluorescence determination of four isoquinoline alkaloids, Talanta 85 (1) (2011) 787–793, https://doi.org/10.1016/j.talanta.2011.04.076.
[32] K. Dong, X.M. Liu, H.F. Dong, X.P. Zhang, S.J. Zhang, Multiscale studies on ionic liquids, Chem. Rev. 117 (10) (2017) 6636–6695.
[33] P.K. Mandal, A. Paul, A. Samanta, Excitation wavelength dependent fluorescence behavior of the room temperature ionic liquids and dissolved dipolar solutes, J. Photochem. Photobiol. Chem. 182 (2006) 113–120, https://doi.org/10.1016/j.jphotochem.2006.01.003.
[34] A.K. Burrell, R.E.D. Sesto, S.N. Baker, T.M. McCleskey, G.A. Baker, The large scale synthesis of pure imidazolium and pyrrolidinium ionic liquids, Green Chem. 9 (2007) 449–454, https://doi.org/10.1039/B615950H.
[35] S. Pandey, S.N. Baker, S. Pandey, G.A. Baker, Fluorescent probe studies of polarity and solvation within room temperature ionic liquids: a review, Journal of Fluorescence 22 (2012) 1313–1343, https://doi.org/10.1007/s10895-012-1073-x.
[36] R. Mercadé-Prieto, L. Rodriguez-Rivera, X.D. Chen, Fluorescence lifetime of Rhodamine B in aqueous solutions of polysaccharides and proteins as a function of viscosity and temperature, Photochem. Photobiol. Sci. 16 (2020) 1727–1734, https://doi.org/10.1039/c7pp00330g.
[37] G. McKay, J.A. Korak, F.L. Rosario-Ortiz, Temperature dependence of dissolved organic matter fluorescence, Environmental science & technology 52 (16) (2018) 9022–9032, https://doi.org/10.1021/acs.est.8b00643.
[38] W.K. Szapoczka, A.L. Truskewycz, T. Skodvin, B. Holst, P.J. Thomas, Fluorescence intensity and fluorescence lifetime measurements of various carbon dots as a function of pH, Sci. Rep. 13 (2023) 10660, https://doi.org/10.1038/s41598-023-37578-z.
[39] T. Wu, H. Pan, R. Chen, D. Luo, H. Zhang, Y. Shen, Y. Li, L. Wang, Effect of solution pH value changes on fluorescence intensity of magnetic-luminescent Fe3O4@Gd2O3:Eu3+ nanoparticles, J. Rare Earths 34 (2016) 71–76, https://doi.org/10.1016/s1002-0721(14)60581-0.
[40] V. Safarifard, Y.D. Farahani, An amine/imine functionalized microporous MOF as a new fluorescent probe exhibiting selective sensing of Fe3+ and Al3+ over mixed metal ions, J. Appl. Organomet. Chem. 2 (2022) 165–179, https://doi.org/10.22034/jaoc.2022.154981.
[41] F. Mohajer, G.M. Ziarani, A. Badiei, New advances on modulating nanomagnetic cores as the MRI-monitored drug release in cancer, J. Appl. Organomet. Chem. 1 (2021) 141–145, https://doi.org/10.22034/jaoc.2021.301405.1032.
[42] R.A. Carpio, L.A. King, R.E. Lindstrom, J.C. Nardi, C.L. Hussey, Density, electric conductivity, and viscosity of several N-alkylpyridinium halides and their mixtures with aluminum chloride, J. Electrochem. Soc. 126 (10) (1979) 1644. https://iopscience.iop.org/article/10.1149/1.2128768/meta.
[43] C. Reichardt, Solvatochromic dyes as solvent polarity indicators, Chem. Rev. 94 (1994) 2319–2358, https://doi.org/10.1021/cr00032a005.
[44] G. Köhler, Solvent effects on the fluorescence properties of anilines, J. Photochem. 38 (1987) 217–238, https://doi.org/10.1016/0047-2670(87)87019-3.
[45] C. Wang, L. Zhang, J.-Y. Wang, S. Su, X.-W. Jin, P.-J. An, B.-W. Sun, Y.-H. Luo, Ultra-thin two-dimensional nanosheets for in-situ NIR light-triggered fluorescence enhancement, FlatChem 24 (2020).
[46] Y.Z. Zheng, N.N. Wang, J.J. Luo, Y. Zhou, Z.W. Yu, Hydrogen-bonding interactions between [BMIM][BF4] and acetonitrile, Phys. Chem. Chem. Phys. 15 (2013) 18055–18064, https://doi.org/10.1039/C3CP53356E.
[47] F. Ilyas, H. Fazal, M. Ahmed, A. Iqbal, M. Ishaq, M. Jabeen, M. Butt, S. Farid, Advances in ionic liquids as fluorescent sensors, Chemosphere 352 (2024) 141434, https://doi.org/10.1016/j.chemosphere.2024.141434.
[48] M.H. Ghatee, M. Zare, F. Moosavi, A.R. Zolghadr, Temperature-dependent density and viscosity of the ionic liquids 1-alkyl-3-methylimidazolium iodides: experiment and molecular dynamics simulation, J. Chem. Eng. Data 55 (9) (2010) 3084–3088, https://doi.org/10.1021/je901092b.